Mustansiriyah Journal of Pure and Applied Sciences

www.MJPAS.com

Performance Evolution Ear Biometrics Based on Features from Accelerated Segment Test

B.A. Mohammed[1] and Z.M. Abood[2]

[1,2]Department Computer science. College of Education, Mustansiriyah University, .Baghdad, Iraq ([1] balkeesahmed2021@uomustansiriyah.edu.iq,
[2] dr.ziadmabood@uomustansiriyah.edu.iq)

A B S T R A C T

In the field of image processing, feature extraction is very important. Various image pre-processing procedures, including scaling, downscaling, resizing, normalization, etc., are applied to the sampled image before features are acquired. Features that would be relevant for image classification and recognition are then extracted using feature extraction methods. Many problems arose in biometric methods (fingerprint, iris, face), which led to the search for new biometrics to identify a person, avoid disease obstacles, continuous change with age, and others. The aim of this work is to present an ear system based on the power extraction of biometric field features of the ear. The proposed system will extract the robust features using the FAST method. This system reduces sprint time while maintaining its accuracy. This is done in two stages, the first stage, is the application of several pre-processing techniques which included the process of a) conversion to grayscale, b) binary filter, c) image brightness, histogram equalization, and image noise reduction. In the second stage, the method of transforming the fixed attribute variable FAST is used to determine the extraction of the force field feature. Where 70**%** images were used for the purpose of training and 30**%** for the purpose of testing. The accuracy of these figures was tested, reaching 95%, and therefore they can be adopted in the classification process in the future by choosing any algorithm.

.**Keywords**: Ear Biometric, Detection technique, FAST Descriptor, Bilateral Filter, Histogram Equalization.

1. Introduction

In general, a biometric system is a pattern recognition system that confirms the user's unique physiological or behavioural characteristics [1]. It is the most dependable and accurate documentation instrument for authenticating human identification in the face of terrorist threats and other criminal actions that jeopardize the safety of countries and peoples [2]. Each biometric has strengths and drawbacks, and no one biometric can be expected to adequately satisfy the needs of all applications [3].

The increased need for safe automated identification systems has fueled research into computer vision and smart systems. Biometrics are used in the majority of human identification systems because of their long-term stability, simplicity of access, and individual uniqueness [4]. The most often used biometrics for human identity include physical or behavioural characteristics such as the face, iris, fingerprint, handprint, hand engineering, sound, and signature. Many biometric system research projects have been successfully realized and are now accessible for general use. These biometric technologies are mostly used for human authentication [5]. Most of these biometrics for human identification need cooperation from the associated individual in order to obtain the biometric features. The whole human population is becoming a mask-wearing community as a result of the present COVID-19 pandemic scenario over the planet. Face recognition systems suffer greatly as a result of this, and current systems must be reworked. Because of the contact-based feature extraction, fingerprint and palmprint recognition is not appropriate in this COVID-19 situation. Because of the sophisticated sensors required to extract the characteristics in Iris, Iris-based recognition systems are expensive. Furthermore, all of the above-mentioned biometric technologies need the person's cooperation in order to be identified. These biometric technologies are less likely to be practical for person identification in densely populated areas such as train stations, museums, retail malls, and so on. As a result, contactless, non-cooperative biometric technology, such as ear biometrics, is required at this time. The human ear retains a stable structure after birth, and it is unique for every individual [6]. Furthermore, the way of obtaining a human ear is contactless and non-intrusive, and it does not need the human participation that we are attempting to identify. In automated identification systems, ear biometrics may supplement other biometric approaches by providing identity signals when other information is inconsistent or even absent. When facial recognition clashes with profile face in surveillance applications, the ear may serve as a source of information regarding the identification of persons in surveillance video. [7] As a result, automatic human identification utilizing ear images is rapidly being researched for possible commercial uses.

The ear is excellent and trustworthy biometry for human verification and identity, and the ear structure is relatively robust and strong in the face of changes in facial expressions or aging[8].

The human ear is one of the finest identifying traits, and it has become crucial due to its employment in extremely sensitive security domains. Uniqueness, permanence, form, and universality are all desirable features of the ear [9]. In general, the look and shape of the ears are unique to each person and reasonably consistent throughout life.[2].

The most visible feature of the ear is the outside border, known as the snail, which merges into the lower lobe. The antihelix is the concha's circular edge that runs parallel to the snail. At the top, it is separated into two branches that generate the upper and lower effects of the counter-snail. Concha is a crust-shaped hollow that connects to an incision. On opposite sides of the incision, there are two little bumps known as antitragus and tragus. A snail crust, the horizontal section of the snail, divides the concha and creates an occasional chain on the concha floor, connecting directly to the snail's crusts, which is part of the snail known as the rising or anterior snail.

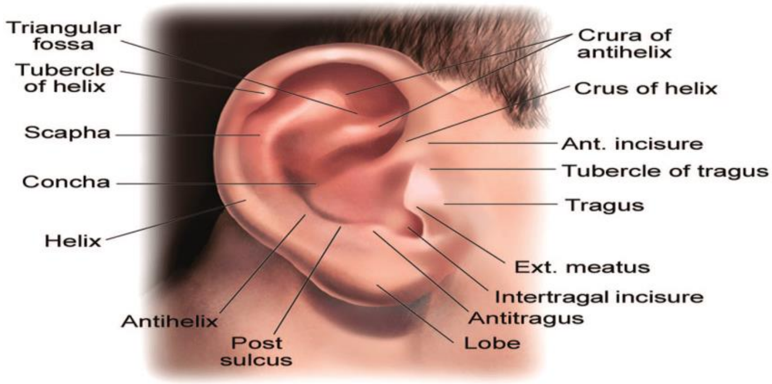

Figure1. Ear human Structure

2. Literature Review

Many researchers were driven to the necessity for ear categorization in the fields of security, general identity verification, and image database investigations. Some of the published work linked to the goals of this project may be found here:

Build a biometric validation framework by using ear images and fingerprints to distinguish a real user. The thinning and binary approach of extracting features are used in the pre-processing phase to enhance all images. The feature extraction technique then adds minutiae and Singular Point fingerprint images to the mix.. Ear features are extracted through the use of powerful feature acceleration (SURF) and powerful, scalable binary key point systems (BRISK). Features are integrated by sequencing fingerprint and ear features for accurate information. Finally, the match is completed through the registration process and the degree of similarity and then by taking advantage of threshold estimates, users are distinguished as real or crooks. Experimental results showed that the proposed multimedia biometrics achieved 95.66% accuracy at an error rate of 0.0434 have been presented [11].

Detailed examination of the extraction of soft biometric variables such as age and sex from each person, aids in many main biometric identification choices as well as improving matching performance.. Many persons included in the ear data set are trained using Gabor extraction of features using a modified version of KNN, and the outcomes are assessed using performance testing based on match ratio against KNN. Detailed examination of the extraction of soft biometric variables such as age and sex from each person, aids in many main biometric authentication choices as well as improves matching effectiveness. has been presented [12].

A combination of traditional ear recognition with soft ear-based biometric features to identify the person. The experiments were conducted on an unrestricted ear database, the AWE database, which contains images collected from the web with a high degree of contrast in relation to post or, lighting and image accuracy. Traditional ear recognition led to correct identification rates of 54.2% and 52.8% for LGBP and BSIF feature carriers. This identification rate increased to 59.5% and 59.2% with the inclusion of soft ear-based biometric features using bayesian fusion have been presented [13].

Proposes putting in place a human ear identification mechanism. Ear recognition, ear extraction, ear identification, and confirmation are the four primary processes of this technique. The proposed system would divide the ear image into leather and non-leather pixels to use a potential skin detector.To complete ear regions, possible image processing through morphological processes. To extract fixed features of the ear, a widely used fixed feature converter is used. Ear recognition has two mechanisms of identification and verification. The Euclidean Distance Scale (EDM) is used to calculate the degree of similarity between the first image in the database and a new image. According to the findings of the three tests done in this research, the accuracy ratio is 100 percent, 92 percent, and 92 percent, respectively. have been presented [14].

A deep, six-layer bypass neural network structure for ear identification. The deep network's potential efficiency is evaluated using the IITD-II ear data set and the ami ear data set. The deep network model obtains a recognition rate of 97.36 percent for the IITD-II data set and 96.99 percent for the AMI data set, respectively. The suggested system's endurance is tested using the AMI Ear data set in an uncontrolled setting. When paired with an adequate monitoring system, this technique may be beneficial in identifying persons in a huge crowd Systems have been presented [15].

3. Features from Accelerated Segment Test (FAST)

FAST is a technique for finding interest spots in an image that was first proposed by Rosten and Drummond [16]. In an image, an interesting point is a pixel with a well-defined location that can be reliably recognized. Interest spots contain a high level of local information value and should preferably be repeated across images [17]. Image matching, object recognition, and tracking are only some of the uses of interest point detection. The concept of interest point detection (also known as corner detection in the literature) is not new. SUSAN corner detector, Moravec corner detection technique, and Harris & Stephens corner detection algorithm are all well-known methods. The FAST approach was designed to construct an interest point detector for real-time frame rate applications like SLAM on a mobile robot with limited computing resources [18].

1. Segment Test Detector

Fast angle detector uses a 16-pixel circle (bresnham circle of 3 radius) to verify whether the p filter point is indeed an angle. Each pixel in the circle is labeled with the right number from 1 to 16 clockwise. If a circle's set of successive N pixels is brighter than the filter pixel p (shown by IP) plus the t threshold value, or each is darker than a p pixel filter minus the t threshold value, then p is designated as a corner. The following are the requirements:

Condition 1: A collection of N continuous pixels S, displaystyle for all xin Sdisplaystyle for all xin S, the intensity of x > Img p + threshold, or displaystyle for all x in Sdisplaystyle for all x in Sdisplaystyle for all x in Sdisplaystyle for all x in Sdisplaystyle for all x in Sdisplaystyle for all xin Img x >Img p+tdisplaystyle Img x>Img p+tdisplaystyle Img x>Img p+tdisplaystyle Img x > Img p+tdisplaystyle Img x >Img p+tdisplaystyle Img x >Img p+tdisplaystyle I

Condition 2: A set of N consecutive pixels S, display style for all xin Sdisplaystyle for all xin Sdisplaystyle for all xin Sdisplaystyle for all xin Sdisplaystyle for all xin Sdisplaystyle for all xin Sdisplaystyle for all xin Sdisplaystyle for all Img xImg p-t, Img xImg p-t, Img xImg p-t, Img xImg p-t, Img x Img p-t, Img x I mg p-t, Img x Img p-t Img x Img p-t Img x Img p-t ,Img x Img p-t Img x Img p-t x.x v Img x.x

If a criteria is satisfied, candidate p may be classed as a corner. It's a compromise to choose N, the number of continuous pixels, and t, the threshold value. On the one hand, the number of selected angle points should not be excessive; rather, it should be enormous. However, excellent performance should not come at the price of computational efficiency. N is generally selected as 12k in the absence of advances in ML. To exclude non-corner locations, a high-speed test policy may be used[19].

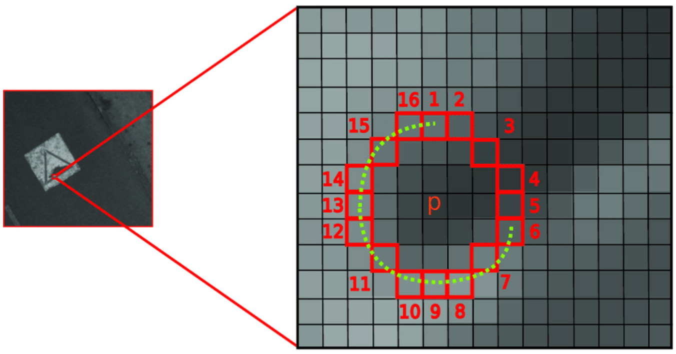

Figure 2.The segment test detector

2. High-speed testing

In the high-speed test, four sample pixels are analyzed to rule out non-angle points: 1, 9, 5, and 13. Because there must be at least 12 brighter or darker pixels in a row, at least three of these four pixels must have a brighter or darker sample than the filter angle. The p filter is not a corner [Ip-t, IP+t] if both I1 and I9 are within. Pixels 5 and 13 are also compared to Ip+t to see if three of them are brighter or darker. The remaining pixels are assessed for final judgment if three of them are brighter or darker than the others. According to the inventor's first publication,[20] verifying the presence of the filtered angle pixels takes an average of 3.8 pixels. When compared to 8.5 pixels per filter angle, a 3.8-pixel drop per filter angle is a considerable improvement in performance.

3. Proposed Method

The proposed system consists of two main parts: the training phase and the testing phase. Each of these stages contains many steps in which ear print samples are processed in a number of ways. Then the FAST method is used to extract the powerful feature from the image, for the same purpose as SIFT technology to reduce processing time, which helps in enhancing detection and matching speed.

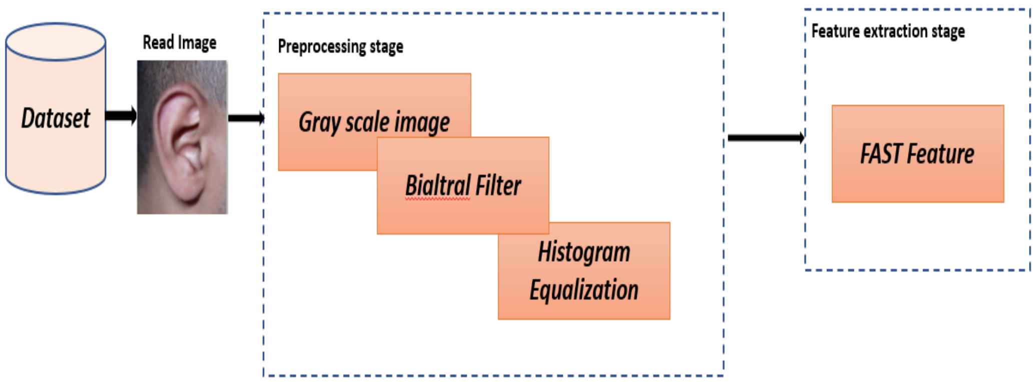

Figure 3. The Ear Biometric Proposal System

3.1 A.Dataset

Esther Gonzalez generated the AMI Ear Dataset while working on her Ph.D. in Computer Science. The photographs were shot in an indoor setting. The database was compiled from 100 distinct participants, all of them were between the ages of 19 and 65. Each subject had seven images collected (six right ear images and one left ear image). The subject sat roughly 2 meters from the camera and stared at some previously set markers in all of the images, which were taken with a Nikon D100 camera under similar lighting conditions. Six of the seven photographs were shot using a 135 mm lens, while the one titled ZOOM was shot with a 200 mm lens. The participant looked forward (FRONTa), up and down (UP, DOWN), and left and right (RIGHT, LEFT) in five of the photos. With the individual looking forward, the sixth photo of the right profile was taken using a different focal length of the camera (ZOOM). The last shot (BACK) was a left-side profile (left ear) with the person staring forward and the same camera focal length as the others. These photos are all in jpeg format and have a resolution of 492702 pixels. Figure (4) is showing the sample of Standard Dataset (AMI Ear Dataset) (7) [19].

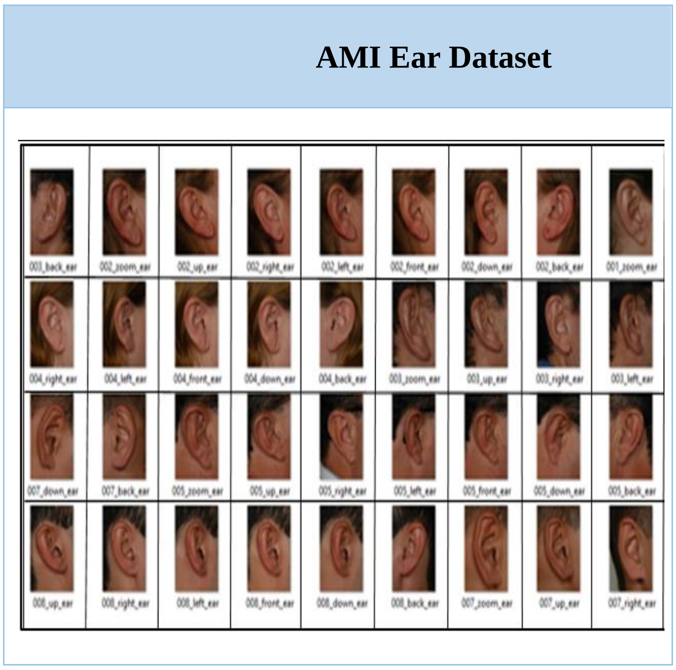

Figure 4. Sample of AMI Ear Dataset.

3.2. Real Database

Balkees Ahmed constructed the genuine database while working on her Master of College of Education, Computer Department. The photographs were shot in an indoor setting. The database was compiled from 40 distinct participants, all of whom were between the ages of two and sixty. Four photos (two right ear images and two left ear images) were collected for each person. All of the photographs were shot using a Sony a7 iii camera under appropriate environmental circumstances in terms of lighting and other factors that cause image data loss, with the subject sitting around 2 meters from the camera. These photographs have a 24-megapixel resolution and are all accessible in jpeg format. Figure (5) is showing a sample of a Real Database.

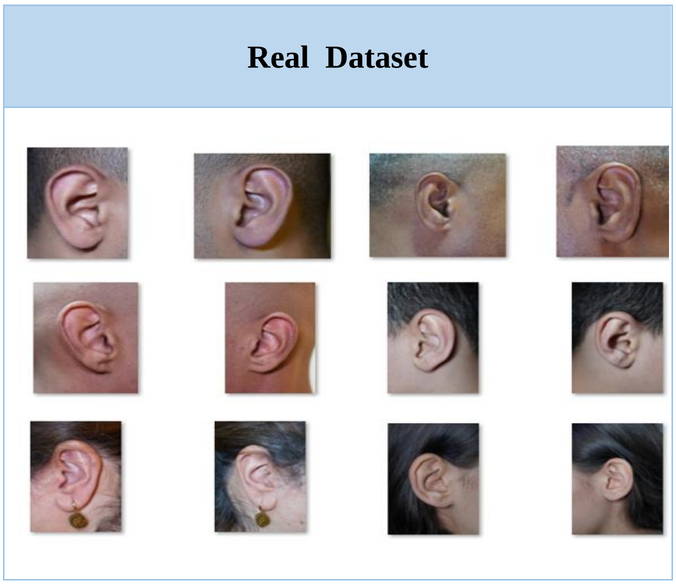

Figure 5. Sample of real Dataset.

3.3 B. Preprocessing phase

It is well understood that most critical approaches for image processing can not start prior to preprocessing is accomplished. Its goal is to enhance the target image so that additional processing produces better results. At this step, the models are subjected to the following preprocessing procedures: The image's noise is removed by using a medium filter contained in the database.

3.4 Convert RGB to Gray Level

In this stage, the RGB colour format of the original input samples is transformed to gray level colour format. This is done to increase model detail perception by stressing the brightness factor, which makes it more accurate and detailed than a traditional gray level format.

3.5 Bilateral Filter

After the grayscale conversion, picture augmentation and noise reduction were necessary while maintaining image accuracy and edges; hence, the bilateral filter was used. Due to numerous iterations and fluctuating pixel density, this modified Gaussian technique was used, in which the filters were enhanced by doubling the use of another Gaussian filter, i.e. pixels with a density near to the ones in the center are only included to calculate an intense density value. As a result, since the following pixels for pixels near the edges are on the other side of the border, significant variations in density appear in a blur when compared to the center pixel, this strategy keeps the ear edges. A linear Gaussian function is used to smooth the data before applying the bilateral filter:

$$g(\mathbf{x}) = (f * G^s)(\mathbf{x}) = \int_{\mathcal{R}} \quad (1) \quad G^s(\mathbf{x}-\mathbf{y})\, d\mathbf{y}$$

The weight for f(y)f(y) = Gs(xy)Gs(xy) and is solely affected by the spatial distance xyxy. The bilateral filter includes a weighting term that is proportional to the whole distance f(y)f(x)f(y)f (x). This has the following consequences:

$$g(\mathbf{x}) = \frac{\int_{\mathcal{R}} f(\mathbf{y})\, G^s(\mathbf{x}-\mathbf{y})\, G^t(f(\mathbf{x}) - f(\mathbf{y}))\, d\mathbf{y}}{\int_{\mathcal{R}} G^s(\mathbf{x}-\mathbf{y})\, G^t(f(\mathbf{x}) - f(\mathbf{y}))\, d\mathbf{y}} \tag{2}$$

4. Histogram Equalization

Histogram equalization is utilized in this technique for ear photos to reduce the influence of varying lighting conditions where photographs are captured. The grayscale image's color histogram is equalized, making the features more discernible by the classifier, and the overall influence of the illumination in the surroundings is eliminated.

4.1 C. FAST Algorithm

The information regarding the features was given in FAST interest Point Detection and point features. We choose the most important features based on a set of criteria and a set of thresholds, and then all features that reflect the most important characteristics of our item of interest, as well as the original image, are returned. Then, from the pixels that surround a focus of interest, feature descriptors, also known as data carrier features, are extracted. Pixels are qualities that are determined by a single point's location. The center placement of neighborhood pixels is determined by this. Finally, we get to the most powerful description. Due to download information that may be recognized and identified, POIs ear image representation points are termed. Finally, it matches features from the first set of coronavirus illness images to the original image's second feature set. The matching step returns indicators for features that are compatible with the pair of features.

This will be illustrated by the algorithm below:

Step1: Choose a pixel "p" on the ear image. Suppose that the intensity of this pixel is IP. This is the pixel that determines whether a pixel is an interesting point or not.

Step 2: Set the T value for the threshold intensity (say 20 percent of the pixel under test).

Step 3: Imagine a 16-pixel circle encircling the pixels.

Step 4: If a pixel is to be identified as a point of interest, "N" out of 16 adjacent pixels must be above or below the IP value T. where N is equal to 12.

Step5: To make the process faster, compare the brightness of the circuit's pixels 1, 5, 9, and 13 to the IP. At least three of these four pixels must fulfill the point of interest presence threshold criteria.

Step6: P is not a point of interest if at least three of the four-pixel values - I_1, I_5, I_9, I_{13} - are not greater or lower than IP + T. (angle). Ignore the pixel as a potential point of interest in this situation. If more than three pixels are above or below Ip + T, examine all 16 pixels to see if 12 adjacent pixels meet the requirement.

Step7: Repeat the technique for all of the pixels in the ear image.

5. Experimental Result.

At this stage, the results obtained from the proposed system will be presented, where two types of datasets were used, one global and the other built, where a group of photos of people of different categories was taken and all permission cases were taken and the images were processed through preprocessing of images where (convert image to grayscale , bilateral filter, and histogram equalization) the strong and distinctive characteristics were extracted through fast algorithm and all the strengths were calculated as shown in Figure (6) and table (1).

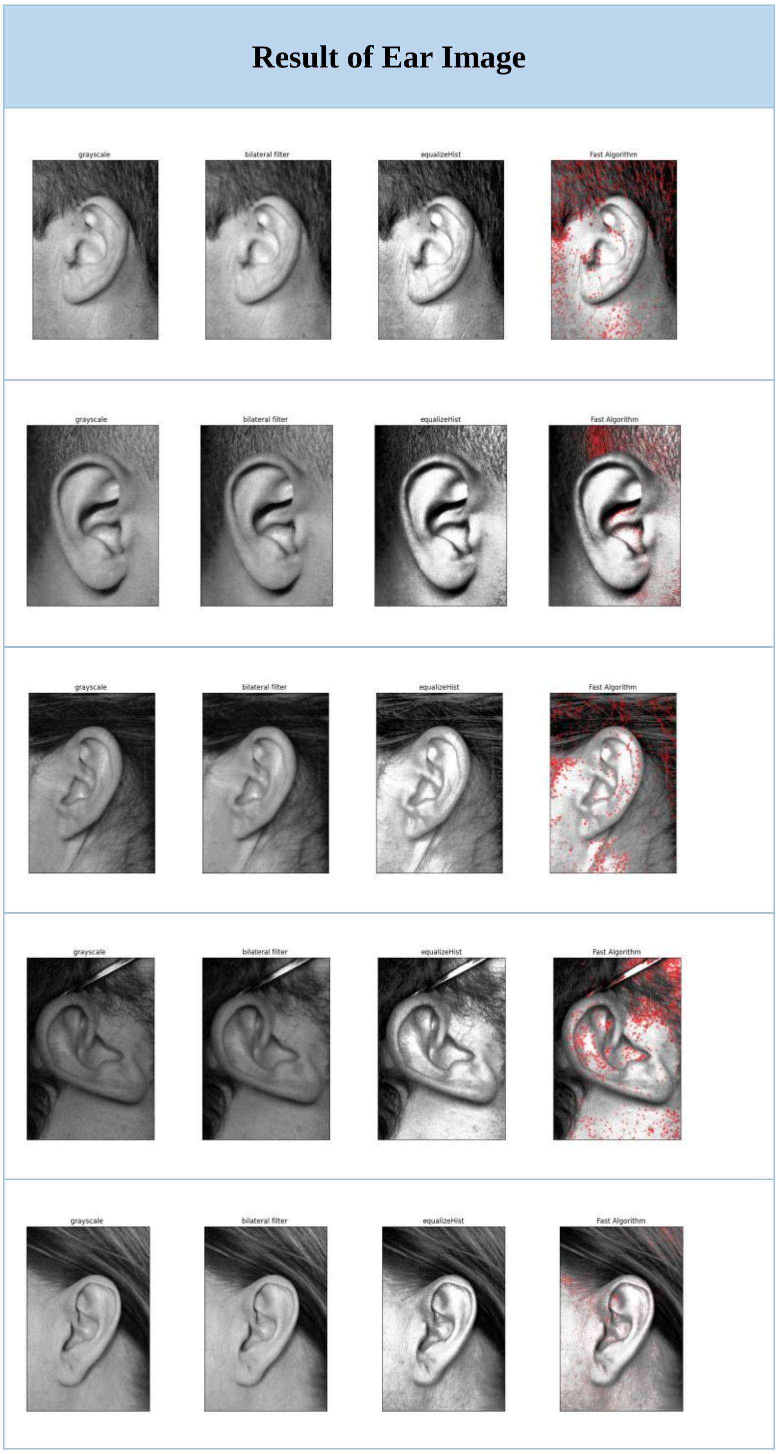

Figure 6. Feature Extraction using the FAST algorithm

Table 1. Feature Vector of ear image

Image	Threshold	Non-Max-suppression	Neighborhood	Total Keypoints With Non Maxsuppression	Total Keypoints Without Non Max Suppression
1	**25**	**True**	**2**	**992**	**992**
2	**25**	**True**	**2**	**4785**	**4785**
3	**25**	**True**	**2**	**79**	**672**
4	**25**	**True**	**2**	**234**	**345**
5	**25**	**True**	**2**	**194**	**456**
6	**25**	**True**	**2**	**46**	**254**
7	**25**	**True**	**2**	**79**	**672**
8	**25**	**True**	**2**	**234**	**345**

6. Conclusion

The FAST method is used to identify and identify the ear print in the scene. In this work, the characteristics of the descriptor were discovered, in addition to our recommended method for the ear print, where two sets of datasets were used, one global and the other built by taking samples for a group of different people using a high specification camera, and a good light environment It contains no noise. The resulting data set corresponding to the ear print in the scene was calculated using three main types of accuracy scales and thresholds to distinguish objects under variable partial occlusion, rotation, lighting conditions, and orientation because the specification is high and the lighting environment is favourable. Using FAST for alignment strengthens the approach. The method was determined to be capable of achieving high accuracy in a small number of training examples. This indicates how robust our feature vector representation is. Furthermore, in the prototype, filtering

FAST points and separate network vectors with lower thresholds enhances the algorithm's overall robustness to rotational shifts and partial occlusion.

7. References

[1] Jain, A. K., Prabhakar, S., Hong, L., & Pankanti, S. (2000). Filterbank-based fingerprint matching. *IEEE transactions on Image Processing*, *9*(5), 846-859.

[2] Kumar, VK Narendira, and B. Srinivasan. "Ear biometrics in the human identification system." International Journal of Information Technology and Computer Science, Volume 4, Issue 2, pp: 41-47, 2012.

[3] Masaoud, K., Algabary, S., Omar, K., Nordin, M. J., & Abdullah, S. N. H. S. (2013). A review paper on ear recognition techniques: models, algorithms and methods. *Australian Journal of basic and applied sciences*, *7*(1), 411-421.

[4] Hurley, D. J., Harbab-Zavar, B., & Nixon, M. S. (2008). Handbook of Biometrics, chapter The ear as a biometric..

[5] Hurley, D. J., Harbab-Zavar, B., & Nixon, M. S. (2008). Handbook of Biometrics, chapter The ear as a biometric.

[6] Yuan, L., & Mu, Z. (2014). Ear recognition based on Gabor features and KFDA. *The Scientific World Journal*, *2014*.

[7] Chen, H., & Bhanu, B. (2007). Human ear detection from 3D side face range images. *3D Imaging for Safety and Security*, 133-155.

[8] Pflug, A., Hartung, D., & Busch, C. (2012). Feature extraction from vein images using spatial information and chain codes. *Information security technical report*, *17*(1-2), 26-35.

[9] Lynch, C. (2000). Ear-prints provide evidence in court. *Glasgow University News*.

[10] Medeiros, M. (2015). Immigration Law-Court of Appeals of Washington Holds Spousal Maintenance Order Not Required to Enforce I-864 Obligation. *Suffolk Transnat'l L. Rev.*, *38*, 221.

[11] Thivakaran, T. K., Chanukya Padira, S. V. V. N., Kumar, A. S., & Reddy, S. S. (2019). Fusion Based Multimodel Biometric Authentication System using Ear and Fingerprint. *International Journal of Intelligent Engineering & Systems*, *12*(1).

[12] Kavipriya, A., & Muthukumar, A. (2019, December). Human Age Estimation based on ear Biometrics using KNN. In *2019 IEEE International Conference on Clean Energy and Energy Efficient Electronics Circuit for Sustainable Development (INCCES)* (pp. 1-5). IEEE.

[13] Joshi, K. V., & Chauhan, N. C. (2011). Edge detection and template matching approaches for human ear detection. In *International Conference on Intelligent Systems and Data Processing (ICISD)* (pp. 50-55).

[14] Hassin, A., & Abbood, D. (2021). Machine Learning System for Human–Ear Recognition Using Scale Invariant Feature Transform. *Artificial Intelligence & Robotics Development Journal*, 1-12.

[15] Ahila Priyadharshini, R., Arivazhagan, S., & Arun, M. (2021). A deep learning approach for person identification using ear biometrics. *Applied intelligence*, *51*, 2161-2172.

[16] Mikolajczyk, K., & Schmid, C. (2002). An affine invariant interest point detector. In *Computer Vision—ECCV 2002: 7th European Conference on Computer Vision Copenhagen, Denmark, May 28–31, 2002 Proceedings, Part I 7* (pp. 128-142). Springer Berlin Heidelberg.

[17] Lowe, D. G. (2004). Distinctive image features from scale-invariant keypoints. *International journal of computer vision*, *60*, 91-110.

[18] Wikipedia, "Corner Detection",< http://en.wikipedia.org/wiki/Corner_detection > ,accessed 16 March 2011.

[19] Rosten, E., & Drummond, T. (2006). Machine learning for high-speed corner detection. In *Computer Vision–ECCV 2006: 9th European Conference on Computer Vision, Graz, Austria, May 7-13, 2006. Proceedings, Part I 9* (pp. 430-443). Springer Berlin Heidelberg.

[20] Koelstra, S., & Patras, I. (2009, May). The fast-3D spatio-temporal interest region detector. In *2009 10th Workshop on Image Analysis for Multimedia Interactive Services* (pp. 242-245). IEEE.